International Journal of Engineering Works
https://www.ijew.io/
ISSN-p: 2521-2419
ISSN-e: 2409-2770
Vol. 9, Issue 10, PP. 173-180 October 2022
https://doi.org/10.34259/ijew.22.910173180

Voltage Source Converter based Grid Integrated Performance of Hybrid Renewable Energy Sources

Muhammad Aurangzeb[1]*, Ai Xin[1], , Muhammad Fawad Chughtai[2], Muhammad Zeshan Afzal[3], Fawwad Hassan Jaskani[4]

[1]State Key Laboratory of Alternate Electrical Power System with Renewable Energy Sources, NCEPU, Beijing, 102206, China

[2]Department of Computer Science and Information Technology, Ghazi University, Dera Gazi Khan, Pakistan

[3]School of Electrical Engineering, Southeast University, Nanjing, 210096, China

[4]Department of Electrical and Electronic Engineering, Faculty of Engineering, Islamia University, Bahawalpur, Pakistan

Maurangzaib42@gmail.com[1]*, aixin@ncepu.edu.cn[1], fawadchughtai5@gmail.com[2], zeshanafzal423@yahoo.com[3], favadhassanjaskani@gmail.com[4]

Received: 11 September, Revised: 03 October, Accepted: 09 October

***Abstract*—** The dynamic stability of grid connected PV, wind and wave power generation system is presented in this paper. The power produced by wind power generation system is design in accordance to Permanent magnet synchronous generator and wave power generation design in linear induction generator. The induction generator works on Archimedes wave swing (AWS) principle. The output terminal of the hybrid system is connected through the common link of dc bus bar via voltage source converter (VSC). Though, this dc power is converted to the ac power through voltage source inverter (VSI). To smoothen the ripple, a supercapacitor (SC) is implied to power supplied to the power grid of distribution side. In this paper a control mechanism is suggested to maintain the balance between the generated side and grid side of the distribution network. In order to achieve the goal, convention tool of stability is applied to the system under various condition of disturbance and approves the effectiveness of the topology used for control and enhance the performance of the hybrid PV and wind generation system.

***Keywords*—** VSC, Renewable Energy, Wind, PV.

I. Introduction

In the ongoing years, the use of non-renewable energy sources like coal, gas, and so forth., increases rapidly because of the expansion in the demand of load on the generating system and it prompts significant issues by making consequences for the nature [1]–[3]. The petroleum products that degrade as they are not inexhaustible in the subsequent few decades. Despite the accessibility of hybrid sources, the interest in energy growth is steadily increased by the public modernization. The pre-eminent arrangement is to use affordable, sustainable energy sources[4]–[7] to meet this need for demand. From the different PV and wind-based texts it is shown that 56 percent of wind energy and 22 percent of solar power supplies in India were generated by a key factor in promoting sustainable energy sources and their interconnection with grid as of 18th May 2018[8]. Solar and wind energy generation was expanded in the main, as the reciprocal accessibility and the output control period of the solar power plant depend on individual sunlight accessibility and wind velocity [10].

Due to the high effect of sustainable energy sources on the climate, discontinuous and irregular voltage results from sources. To ease this progress, power sources are combined to identify the renewable energy network and MPPT control computing is needed to monitor the most extraordinary power sources[11]. The basic structure of a sustainable energy hybrid topology is shown in Fig.1. Other MPPT experiments have included: dislocation and observation (P&O), hill climbing, Fuzzy command, hybrid system and artificial neural network open to maximum energy independence from economical renewable sources[12]. On the other hand, a design and style optimization approach for the new major grid-connected Voltaic Power Generation System, which focused on a multi-faceted innate algorithm, was shown in the new development of the large standalone wind-photovoltaic system [11]. The system was a stand-alone photovoltaic battery hybrid power generation system. The dynamic stability of a macro grid that connects with a wind transformer, a simultaneous diesel dynamo and a cellular energy storage repository was investigated in [22], while in the new HPGS grid-connected PV-diesel power station, which uses a further wave in the PV handle curve, the smaller wave solidity development outcomes were presented [13].

To enhance the efficiency of a photovoltaic and wind energy with battery HPGS, the creators in [14] put forward a narrative hold strategy built on the particular circumstance of charge associated with the battery. The use of a SMEs to improve the dynamic certainty of the grid-affixed wind-photo voltaic hybrid power generation system throughout the matrix energy sink has been researched in [15] as the power stabilizing of a hybrid macro grid using Super Capacitors was documented in [16]. Even though a great deal regarding outstanding analysis within the matters of WPG methods (Wave Power Generation Systems) have been performed and detailed in [17]-[29], the blend of the wind power generation systems together with the other RESs in typically the HPGSs has not recently been broadly examined. Only a new handful of issued papers in particular [30]-[32] has announced regarding the hybrid power generation systems together with the wind energy.

The combination of wave turbine and wind energy engendering techniques utilizing a dc macro grid was deliberated and detailed in [30] while a mixture of quartet various wave power transformation tools fastened to a diffusion department was constituted in [31]. The authors in [32] had expanded an autonomous Photo Voltaic-wind hybrid sustainable energy origination structure for use in islands in Malaysia. In that fusion project, the WPGS was replicated by a Permanent Magnet Synchronous Generator operated by a swaying aqua upright appliance and the turbine was utilized as a reinforcement power-depot order. Within this paper, the energetic stableness examined outcomes of a new matrix-linked wind and photovoltaic HPGS through the supercapacitor regarding smoothing the strength variations are conferred. A new command strategy is recommended to smoothen the power provided to the grid, also, to continue the well-balanced functioning of the considered method while drawing out the highest strength from wave along with the PV exhaustible means. Typically the presentation of the researched arrangement and the performance in the SC united together with the offered power structure are inspected along the root-loci survey outcomes of the process inherent value in addition to the measure-original outputs.

II. METHODOLOGY

In this section, we are going going to discuss about wave energy, wind energy and solar energy. Design parameters and techniques used in the design of wave, wind and solar also mentioned. In wave generator we perform parks and Clarke transformation and inverse of these transformations for abc to measurements. A 100 kilowatt of wave generation, 10 kw of wind and 20 kilowatt of solar energy is successfully integrated with the utility grid. The synchronizing voltage and current also plotted. The grid side response and load response plotted and discussed. Mathematical modeling is also explained in this chapter that how we transform abc to $dq0$ transformation. In wind system, rotor current, rotor speed and irradiance effect on the system is described and mppt signal is controlled to get the maximum power all the time.
The presented model is shown in figure 1, which is given below.

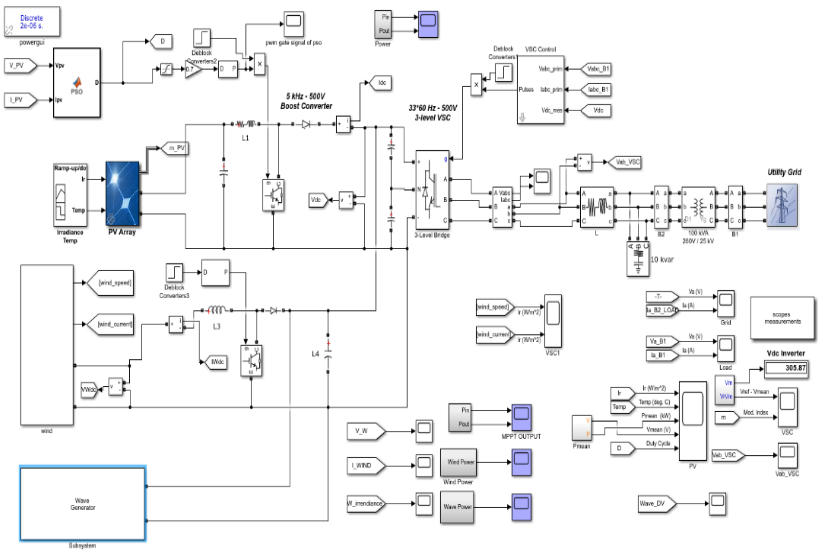

Fig 1. Presented Simulink Model

In many developing countries, the development of islands is almost affined to availability of electric power cause many islands over the country where electric power grid is unavailable and the electricity is generated by traditional energy sources, but the main problem is to increase fuel cost remotely. Even, the electricity is generated by conventional sources increases the million tons of CO_2, which increases global warming.

To overcome this challenge, renewable energy sources is the only the solution, solar energy is an environment friendly energy source. The main problem with solar energy is dependency on environment conditions, doesn't produce power during night and cloudy periods. It means solar system doesn't produce power continuously at load. This issue can be solved by integrating the solar system with another renewable energy sources or storage system like wind, wave, fuel cell, battery bank etc to form a hybrid system.

Wave Energy i.e. Ocean Wave Energy uses surface wave power to generate electricity. Even many wave energy conversion techniques have been used. Here we use Archimedes Wave Swing (AWS)conversion technique.

Principle of Working (Wave)

$$P = \frac{\rho g^2}{64\pi} H_{m0}^2 T_e \approx \left(0.5 \frac{kw}{m^3.s} \right) H_{m0}^2 T_e \quad (1)$$

Where,
P= Wave Energy Flux
ρ = Water Density
g = Acceleration by Gravity
H_{m0}^2 = Significant Wave Height
T_e = Wave energy Period

In other hand, we can also find the wave energy and its flux.

$$P = \frac{1}{16} \rho g H_{m0}^2 \quad (2)$$

As the wave propagates, the energy of the wave is transported. The transported velocity is the group velocity. Through a vertical plane, the energy flux will be:

$$P = Ec_g \quad (3)$$

c_g = Group Velocity.

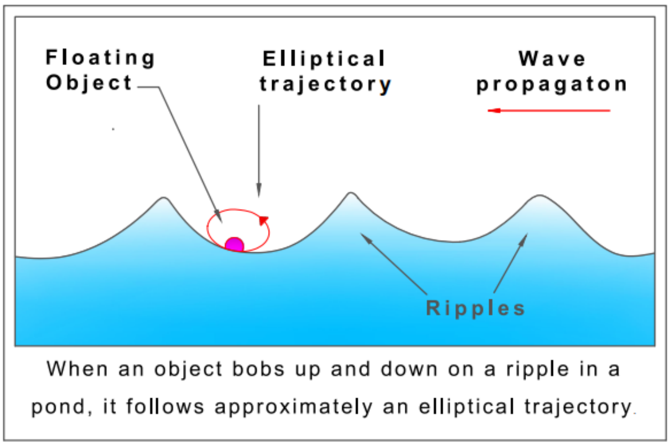

(a)

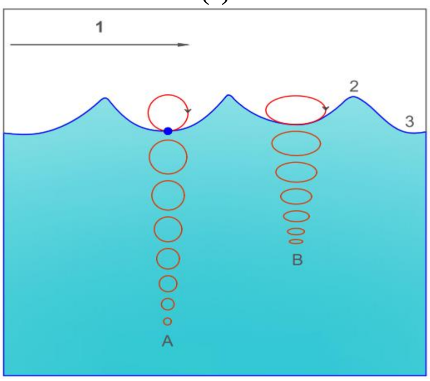

(b)

Figure 2,(a)(b): Motion of a Particle in an ocean Wave

A is representing the elliptical motion in deep Water
B is representing the shallow water

Simulink Model of Wave Generator

Wave generator is validated in Matlab/Simulink as shown in the picture below. The main part in this design is $abc\ to\ dq0$ transformation. Park and Clarke Transformation are the major transformation in this model and also inverse of park and Clarke transformation. You can see the method used in this model. Mathematical modeling of $abc\ to\ dq0$ transformation is also discussed below.

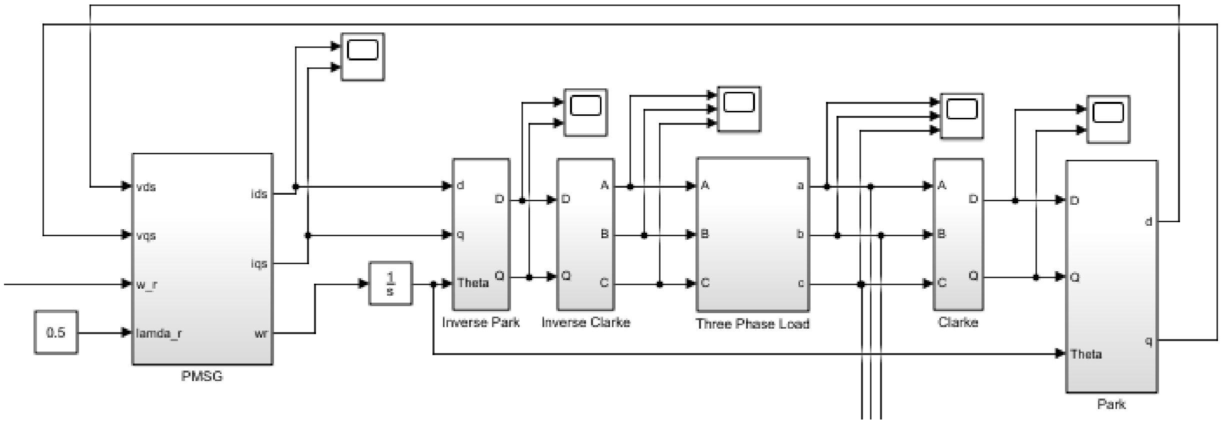

Figure 3: Simulink view of wave generator

For performing the $qd0$ transformation, multiply transformation matrix K by machine variables [18]. As our interest is to transform stator variables to rotor reference frame, the electrical rotor angle (θ_{re}) can be used as reference in transformation and transformation matrix K_s^r where,

$$K_s^r = \frac{2}{3}\begin{bmatrix} \cos(\theta_{re}) & \cos\left(\theta_{re} - \frac{2\pi}{3}\right) & \cos\left(\theta_{re} + \frac{2\pi}{3}\right) \\ \sin(\theta_{re}) & \sin\left(\theta_{re} - \frac{2\pi}{3}\right) & \sin\left(\theta_{re} + \frac{2\pi}{3}\right) \\ \frac{1}{2} & \frac{1}{2} & \frac{1}{2} \end{bmatrix} \quad (4)$$

The recent stator variables in $qd0$ transformation are now given as

$$f_{qd0s}^r = \begin{bmatrix} f_{qs}^r \\ f_{ds}^r \\ f_{0s}^r \end{bmatrix} \quad (5)$$

And

$$f_{qd0s}^r = K_s^r f_{abcs} \quad (6)$$

Figure 5 shows recent q and d axes in rotor reference frame. It is observed that $q-axis$ and $d-axis$ are 90° apart. The $q-axis$ is referenced by θ_{rm}; and is having effect of inverting sine and cosine terms in equations.

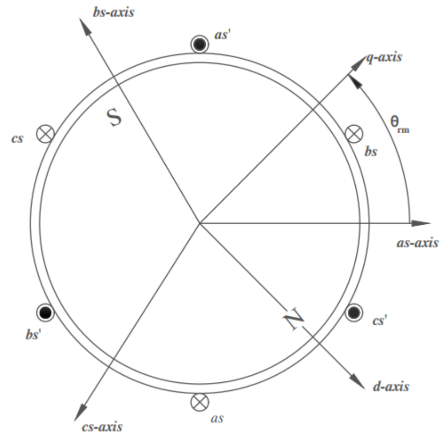

Figure 4, Three-phase non-salient PMSM Cross section with q and d axes

The inverse transformation matrix $(K_s^r)^{-1}$ is used to revert from $qd0$ to abc variables, where

$$f_{abcs} = (K_s^r)^{-1} f_{qd0s}^r \quad (7)$$

and

$$(K_s^r)^{-1} = \begin{bmatrix} \cos(\theta_{re}) & \sin(\theta_{re}) & 1 \\ \cos\left(\theta_{re} - \frac{2\pi}{3}\right) & \sin\left(\theta_{re} - \frac{2\pi}{3}\right) & 1 \\ \cos\left(\theta_{re} + \frac{2\pi}{3}\right) & \sin\left(\theta_{re} + \frac{2\pi}{3}\right) & 1 \end{bmatrix} \quad (8)$$

Efficiency of Wind turbine

While converting mechanical energy into electrical energy, the available partial power in wind is converted [28]. The ratio of wind turbine power and power available in wind is called the overall efficiency of wind turbine, is given as,

$$\eta_{total} = \frac{P_{Out}}{P_{Input}} \tag{9}$$

The wind turbine contains two types of efficiency: first is rotor efficiency (C_P) i.e. power coefficient and second is generator efficiency (η). The wind turbine rotor efficiency depends on the rotor blades design. Secondly, the generator efficiency depends upon the generator electrical design. The output power of the generator is given as:

$$P_{output} = \rho A v^3 C_p \eta \tag{10}$$

To get the rotor efficiency the mechanical power $(P_{mechanical})$ of the rotor has to be calculated. It can be calculated by measuring the rotational speed (ω) as well as the mechanical torque (T) of the rotor. So, mechanical power can be calculated as:

$$P_{mechanical} = T\omega \tag{11}$$

Where T is the mechanical torque of the rotor (Nm) and ω is the rotational speed of the rotor (rad/s).

III. Results

Grid end power

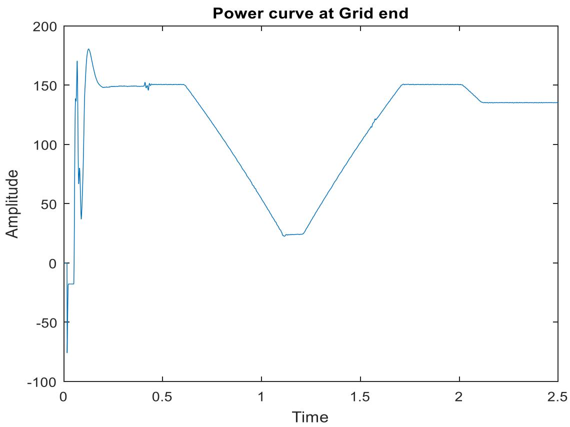

Figure 5: Grid Power in KW

The above mentioned graph represent the variation in Grid side Solar Power due to variation of Solar Irradiance. Initially the solar power is 0 kW then it decreases to -50 kW at time 0.1sec , it increases to 140kW and decreases to 40 kW again increases to 180 kW very instantly for time interval 0.1 sec to 0.2 sec then drastically it decreases to 150 kW at time 0.3 sec ,now it remain constant upto 0.6 sec, again it decreases to 25kW and remain constant for time interval 1.2 sec-1.3 sec, again it increases up to 150 kW and remain constant for time interval 1.6 sec - 2.1sec again it decreases to140kW and remain constant for time interval 2.2 sec - 2.5 sec.

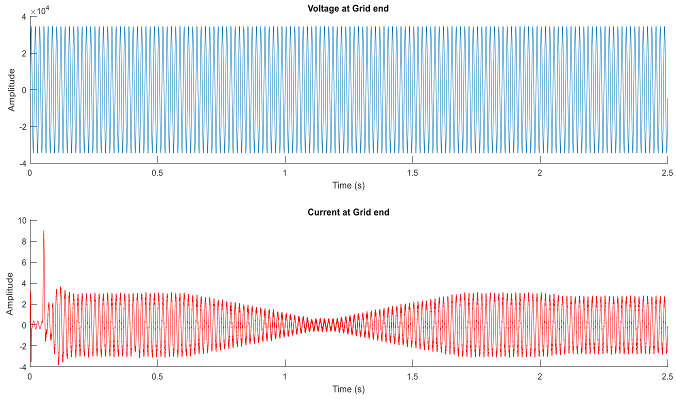

Figure 6: Grid side voltage and Current

The Voltage remains constant and current varies due to Solar Irradiance w.r.t. time at grid end.

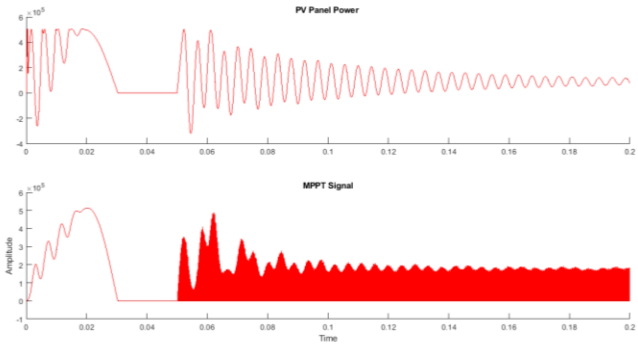

Figure 7: PV power vs MPP Signal

Reference Voltage and Modulation Index

In below figure Graph shows the variations in reference voltage w.r.t. time. Initially it is 0.1V then it increases drastically up to 560V at time 0.1 sec again it decreases drastically up to 370V at time 0.2 sec ,it increases up to 555V at time 0.3 sec, again it decreases gradually up to 500V at time 0.32 sec now it remain constant up to 2.5 sec.

Graph 2 shows the variation in Modulation Index w.r.t. time.

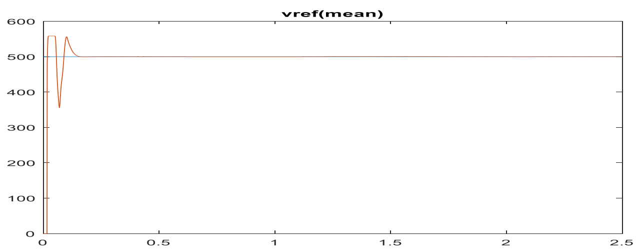

(a)

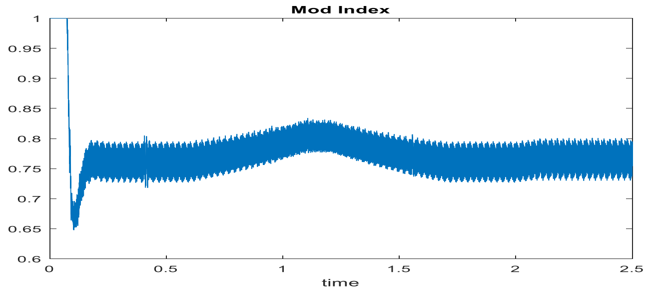

(b)

Figure 8: (a) and (b) Variations in Reference Voltage and Modulation Index w.r.t. time

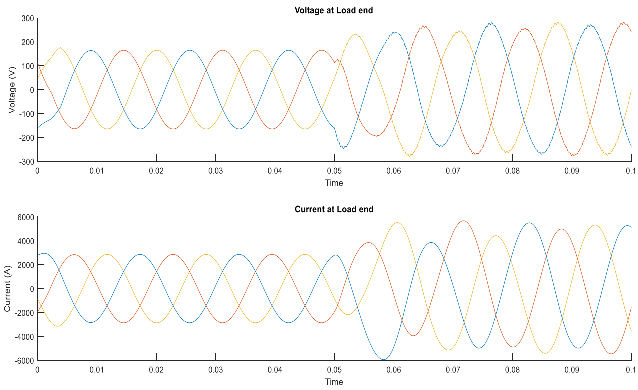

Figure 9: Load side response

Load side response is shown in fig 9 and three phase voltage and current waveform are displayed. A little distortion at the time interval of 0.05 to 0.06 sec.

Variable Voltages of Stator Machine

The stator flux linkage, is depicted in Figure 10, where the system response is seen in (a) and a more detailed view of the waveforms is seen in (b) with the differences coming from the flux produced by currents in the stator windings. The waveforms for vabcs can also be seen. The stator currents iabcs are also on display in these figures. The current waveform shape is caused from a combination of factors, but they are largely controlled by the effects of the diode rectifiers which are feeding a common dc bus

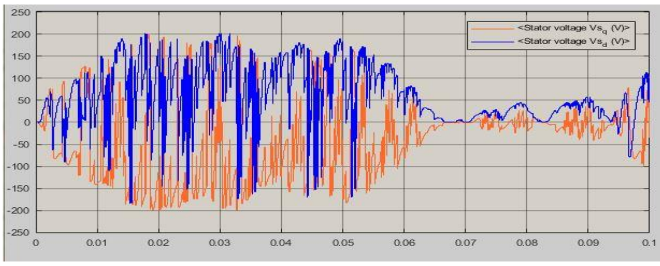

(a) Stator machine variables Stator voltages vabcs .

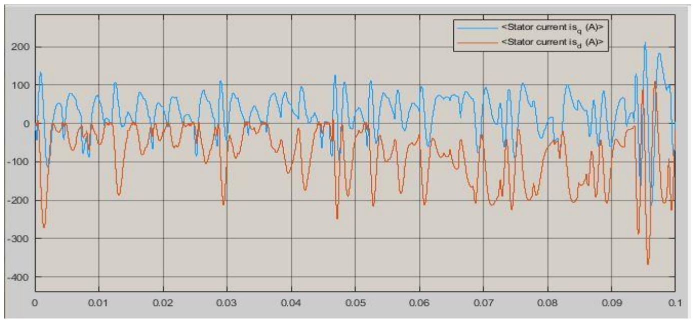

b) Variable Stator Current of Stator machine Obtained from Clarke Transformation

Figure 10 (a) (b)

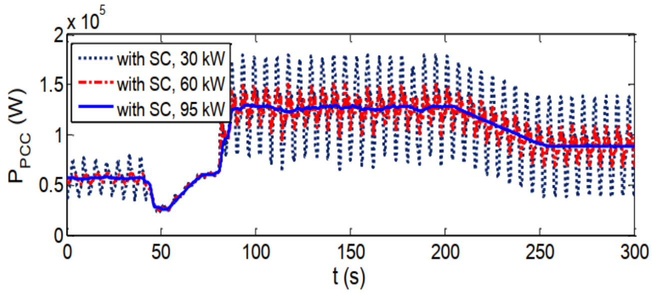

Figure 11: size of the utilized Super Capacitor

The result of the size of the utilized Super Capacitor on the efficiency of the analyzed method is evaluated. About three various Super Capacitors along with the energy evaluations of the 60 kW, 30 kW, and also 95 kW, are usually in turns utilized for the analyzed method. the relative dynamic reactions of the energetic energy given to the supply power main grid for about three various energy evaluations of the utilized Super Capacitor. This is visible through the plots proven in Fig.11 that as soon as the size of the utilized Super Capacitor is enhanced, the energetic energy given to the supply power main grid is finer, that illustrates the additional development in the efficiency of the analyzed method in case the greater Super Capacitor is utilized.

Wave dc bus voltage

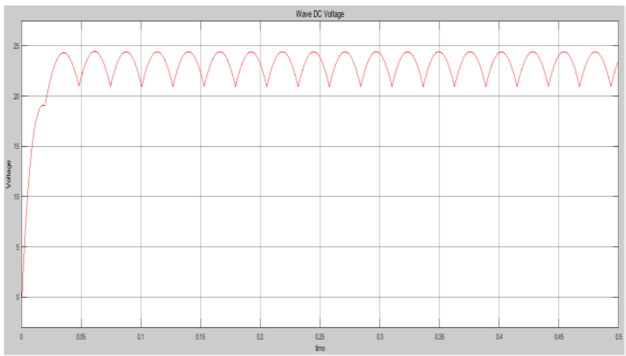

Figure 12: DC bus voltage

The DC bus voltage of wave is shown here in fig 12. The voltage is almost fixed to 24V for entire duration of 0.5 with little change initially.

Power of wave

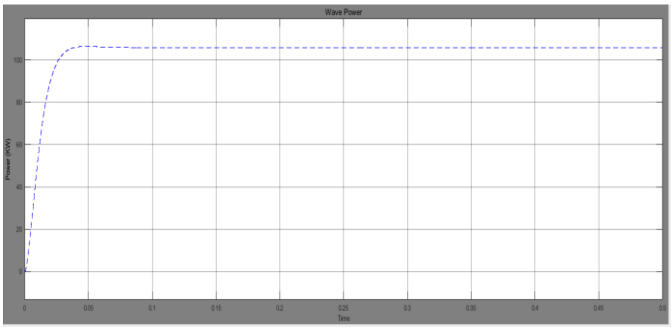

Figure 13: Wave power

In the above figure, wave power is shown for the entire time period. Design of the wave generator was 100 kw. At the start power spikes but after that system is showing stable100 kw approximately.

In figure 14, the photovoltaic irradiance at the range of solar cell is issued to the variants as demonstrated in Fig.14(a) while the wave energy is retained at the maximum intensity of 0.4 MN together with an interval of 10 seconds. The variants of the solar power irradiance are likewise supposed to consist of the substantial-consistency imbalances because of the rapid transforming of the local meteorological circumstances.

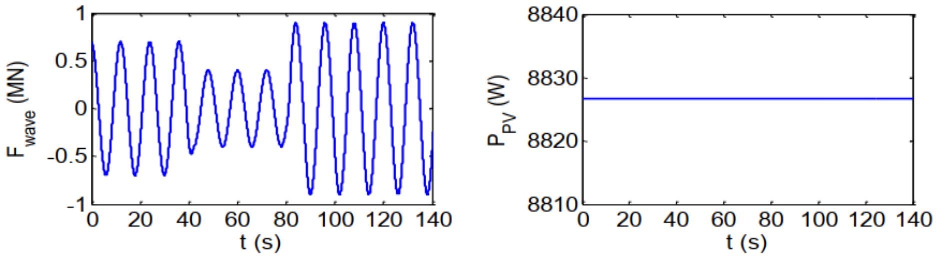

(a) Wave force (b) P_{PV}

Figure 14: Wave Force and PV Power

CONCUSLION

The detail study about stability of hybrid PV, Wave and wind energy system interlinked to grid has been given. A storage system for energy based on supercapacitor has been used to minimise the fluctuation of connected grid system. Moreover, to maintain the balance operation and achieving maximum power from the hybrid system connected to the grid, a control technique is suggested. Both root loci and time-domain analysis of the mentioned system are performed to check the dynamic efficiency under different operating conditions. It can be summarized from outputs of the suggested control technique has the capability to maintain the balance operation of mentioned system.

REFERENCES

[1] M. A. Hannan, Z. A. Ghani, M. M. Hoque, P. J. Ker, A. Hussain and A. Mohamed, "Fuzzy Logic Inverter Controller in Photovoltaic Applications: Issues and Recommendations," in IEEE Access, vol. 7, pp. 24934-24955, 2019, doi: 10.1109/ACCESS.2019.2899610.

[2] S. Iqbal, A. Xin, M. U. Jan, H. Rehman, S. Salman, and S. A. Abbas Rizvi, "Improvement in the Efficiency of Inverter Involved in Microgrid," 2018 2nd IEEE Conference on Energy Internet and Energy System Integration (EI2), Beijing, 2018, pp. 1-5.

[3] L. Chen et al., "Study of Modified Flux-Coupling-Type SFCLs For Stability Improvement of a Multi-Machine Power System Based On Energy Function," in IEEE Transactions on Applied Superconductivity, vol. 31, no. 8, pp. 1-7, Nov. 2021, Art no. 0500207, doi: 10.1109/TASC.2021.3091040.

[4] M. Z. Malik, A. Ali, G. S. Kaloi, A. M. Soomro, M. H. Baloch, and S. T. Chauhdary, "Integration of Renewable Energy Project: A Technical Proposal for Rural Electrification to Local Communities," *IEEE Access*, vol. 8, pp. 91448–91467, 2020, doi: 10.1109/ACCESS.2020.2993903.

[5] S. Iqbal et al., "Feasibility Study and Deployment of Solar Photovoltaic System to Enhance Energy Economics of King Abdullah Campus, University of Azad Jammu and Kashmir Muzaffarabad, AJK Pakistan," in IEEE Access, vol. 10, pp. 5440-5455, 2022, doi: 10.1109/ACCESS.2022.3140723.

[6] R. M. Elavarasan *et al.*, "A Comprehensive Review on Renewable Energy Development, Challenges, and Policies of Leading Indian States with an International Perspective," *IEEE Access*, vol. 8, pp. 74432–74457, 2020, doi: 10.1109/ACCESS.2020.2988011.

[7] S. Iqbal, A. Xin, M. U. Jan, and M. A. Abdelbaky, "Improvement of Power Converters Performance by an E ffi cient Use of Dead Time Compensation Technique," *Appl. Sci.*

[8] Z. Shu, Y. Chen, C. Deng, F. Zheng and H. Zhong, "Pareto Optimal Allocation of Flexible Fault Current Limiter Based on Multi-Objective Improved Bat Algorithm," in IEEE Access, vol. 9, pp. 12762-12778, 2021, doi: 10.1109/ACCESS.2021.3050795.

[9] S. Iqbal, S. Habib, N.H. Khan, M. Ali., M. Aurangzeb, and Ahmed, E.M., 2022. Electric Vehicles Aggregation for Frequency Control of Microgrid under Various Operation Conditions Using an Optimal Coordinated Strategy. *Sustainability*, *14*(5), p.3108.

[10] L. Chen et al., "Performance Analysis of an Improved Flux-Coupling-Type SFCL in a Medium-Voltage Wind Turbine Generation System," in IEEE Transactions on Applied Superconductivity, vol. 31, no. 8, pp. 1-6, Nov. 2021, Art no. 0500406, doi: 10.1109/TASC.2021.3091079.

[11] S. Iqbal *et al.*, "Role of Power Electronics in Primary Frequency Control and Power Quality in an Industrial Micro-grid Considering V2G Technology," *2019 IEEE 3rd Conference on Energy Internet and Energy System Integration (EI2)*, 2019, pp. 1188-1193, doi: 10.1109/EI247390.2019.9062071.

[12] M. Aurangzeb, A. Xin, S. Iqbal and M. U. Jan, "An Evaluation of Flux-Coupling Type SFCL Placement in Hybrid Grid System Based on Power Quality Risk Index," in IEEE Access, vol. 8, pp. 98800-98809, 2020, doi: 10.1109/ACCESS.2020.2996583.

[13] H. Ur Rehman, X. Yan, M. A. Abdelbaky, M. Ullah Jan, and S. Iqbal, "An advanced virtual synchronous generator control technique for frequency regulation of grid-connected PV system," *Int. J. Electr. Power Energy*

Syst., vol. 125, no. June 2020, p. 106440, 2021, doi: 10.1016/j.ijepes.2020.106440.

[14] A. Raheem *et al.*, “Renewable energy deployment to combat energy crisis in Pakistan,” *Energy. Sustain. Soc.*, vol. 6, no. 1, 2016, doi: 10.1186/s13705-016-0082-

[15] S. Agrawal, S. K. Vaishnav, D. K. Yadav and R. K. Somani, "Power Quality Enhancement of Soft Computing FLC MPPT Based Standalone Photovoltaic System," 2019 2nd International Conference on Power Energy, Environment and Intelligent Control (PEEIC), 2019, pp. 429-434, doi: 10.1109/PEEIC47157.2019.8976533.

[16] S. Iqbal *et al.*, “Aggregation of EVs for Primary Frequency Control of an Industrial Microgrid by Implementing Grid Regulation Charger Controller,” *IEEE Access*, vol. 8, pp. 141977–141989, 2020, doi: 10.1109/ACCESS.2020.3013762.

[17] C. R. Charan, K. N. Sujatha and K. P. Satsangi, "Fuzzy logic controller based model for rooftop/grid connected solar photovoltaic system," 2016 IEEE Region 10 Humanitarian Technology Conference (R10-HTC), 2016, pp. 1-6, doi: 10.1109/R10-HTC.2016.7906837.

[18] P. K. Ray, S. R. Das and A. Mohanty, "Fuzzy-Controller-Designed-PV-Based Custom Power Device for Power Quality Enhancement," in IEEE Transactions on Energy Conversion, vol. 34, no. 1, pp. 405-414, March 2019, doi: 10.1109/TEC.2018.2880593.

[19] M. Aurangzeb, X. Ai, M. Hanan, M. U. Jan, H. Ur Rehman and S. Iqbal, "Single Algorithm Mpso Depend Solar And Wind Mppt Control And Integrated With Fuzzy Controller For Grid Integration," 2019 IEEE 3rd Conference on Energy Internet and Energy System Integration (EI2), 2019, pp. 583-588, doi: 10.1109/EI247390.2019.9061805.

[20] A. Kumar and P. Kumar, "Power Quality Improvement for Grid-connected PV System Based on Distribution Static Compensator with Fuzzy Logic Controller and UVT/ADALINE-based Least Mean Square Controller," in Journal of Modern Power Systems and Clean Energy, vol. 9, no. 6, pp. 1289-1299, November 2021, doi: 10.35833/MPCE.2021.000285.

[21] M. U. Jan, A. Xin, H. U. Rehman, M. A. Abdelbaky, S. Iqbal and M. Aurangzeb, "Frequency Regulation of an Isolated Microgrid With Electric Vehicles and Energy Storage System Integration Using Adaptive and Model Predictive Controllers," in IEEE Access, vol. 9, pp. 14958-14970, 2021, doi: 10.1109/ACCESS.2021.3052797.

[22] L. Farah, A. Hussain, A. Kerrouche, C. Ieracitano, J. Ahmad and M. Mahmud, "A Highly-Efficient Fuzzy-Based Controller With High Reduction Inputs and Membership Functions for a Grid-Connected Photovoltaic System," in IEEE Access, vol. 8, pp. 163225-163237, 2020, doi: 10.1109/ACCESS.2020.3016981.

[23] M. U. Jan, A. Xin, M. A. Abdelbaky, H. U. Rehman and S. Iqbal, "Adaptive and Fuzzy PI Controllers Design for Frequency Regulation of Isolated Microgrid Integrated With Electric Vehicles," in IEEE Access, vol. 8, pp. 87621-87632, 2020, doi: 10.1109/ACCESS.2020.2993178.

[24] P. K. Pardhi, S. K. Sharma and A. Chandra, "Control of Single-Phase Solar Photovoltaic Supply System," in IEEE Transactions on Industry Applications, vol. 56, no. 6, pp. 7132-7144, Nov.-Dec. 2020, doi: 10.1109/TIA.2020.3024171.

[25] M. B. Shadmand and R. S. Balog, “Multi-objective optimization and design of photovoltaic-wind hybrid system for community smart dc microgrid,” IEEE Trans. Smart Grid, vol. 5, no. 5, pp. 2635-2643, Sep. 2014.

[26] N. Patel, N. Gupta, and B. C. Babu, “Photovoltaic System Operation as DSTATCOM for Power Quality Improvement Employing Active Current Control,” *IET Generation, Transmission & Distribution*, May 2019.

[27] N. Patel, A. Kumar, N. Gupta, S. Ray, and B. C. Babu, “Optimized PI-4VPI Current Controller for Three-Phase Grid-integrated Photovoltaic Inverter under Grid Voltage Distortions,” *IET Renewable Power Generation*, vol. 14, no. 5, pp. 779-792, Nov. 2019.

[28] S. Mishra and D. Ramasubramanian, “Improving the small signal stability of a PV-DE-dynamic load-based microgrid using an auxiliary signal in the PV control loop,” IEEE Trans. Power Systems, vol. 30, no.1, pp. 166-176, Jan. 2018.

[29] X. Li, D. Hui, and X. Lai, “Battery energy storage station (BESS)-based smoothing control of photovoltaic (PV) and wind power generation fluctuations,” IEEE Trans. Sustainable Energy, vol. 4, no. 2, pp. 464- 473, Apr. 2016.

[30] S.-T. Kim, B.-K.Kang, S.-H.Bae, and J.-W. Park, “Application of SMES and grid code compliance to wind/photovoltaic generation system,” IEEE Trans. Applied Superconductivity, vol. 23, no. 3, pp. 5000804, Jun. 2018.

[31] J. Khan and U. Nasir, “Voltage stabilization of hybrid micro-grid using super capacitors,” J. Power and Energy Engineering, vol. 3, no. 6, pp. 1-9, Jun. 2015.

[32] S. Ceballos, J. Rea, I. Lopez, J. Pou, E. Robles, and D. L. O’Sullivan, “Efficiency optimization in low inertia Wells turbine-oscillating water column devices,” IEEE Trans. Energy Conversion, vol. 28, no. 3, pp. 553-564, Sep. 2017.

How to cite this article:

Muhammad Aurangzeb, Ai Xin, , Muhammad Fawad Chughtai, Muhammad Zeshan Afzal, Fawwad Hassan Jaskani “Voltage Source Converter based Grid Integrated performance of Hybrid Renewable Energy Sources”, International Journal of Engineering Works, Vol. 9, Issue 10, PP. 173-180, October 2022. https://doi.org/10.34259/ijew.22.910173180.